(5) M. J. Bennett, K. G. Caulton, and F. A. Cotton, *Inorg. Chem.*, **8**, 1 (1969).
(6) F. A. Cotton and M. Jeremic, *Synth. Inorg. Met.-Org. Chem.*, **1**, 265 (1971).
(7) (a) G. Albrecht and D. Stock, *Z. Chem.*, **7**, 321 (1967); (b) T. Aoki et al., *Bull. Chem. Soc. Jpn.*, **42**, 545 (1969); (c) J. Krausse, G. Marx, and G. Schodl, *J. Organomet. Chem.*, **21**, 159 (1970); (d) F. A. Cotton et al., *Acta Crystallogr., Sect. B*, **27**, 1664 (1971).
(8) (a) D. Lawton and R. Mason, *J. Am. Chem. Soc.*, **87**, 921 (1965); (b) J. V. Brencic and F. A. Cotton, *Inorg. Chem.*, **8**, 7 2698 (1969); **9**, 346, 351 (1970); (c) F. A. Cotton and J. R. Pipal, *J. Am. Chem. Soc.*, **93**, 5441 (1971); (d) F. A. Cotton and J. G. Norman, Jr., *ibid.*, **94**, 5697 (1972); *J. Coord. Chem.*, **1**, 161 (1972); (e) C. L. Angell, F. A. Cotton, B. A. Frenz, and T. R. Webb, *J. Chem. Soc., Chem. Commun.*, 399 (1973); (f) F. A. Cotton, B. A. Frenz, and T. R. Webb, *J. Am. Chem. Soc.*, **95**, 4431 (1973).
(9) J. G. Norman, Jr., and H. J. Kolari, *J. Am. Chem. Soc.*, **97**, 33 (1975).
(10) J. G. Norman, Jr., and H. J. Kolari, *J. Chem. Soc., Chem. Commun.*, 649 (1975).
(11) A. P. Mortola, J. W. Moskowitz, N. Rosch, C. D. Cowman, and H. B. Gray, *Chem. Phys. Lett.*, **32**, 283 (1975).
(12) F. A. Cotton, B. A. Frenz, J. R. Ebner, and R. A. Walton, *J. Chem. Soc., Chem. Commun.*, 4 (1974).
(13) J. R. Ebner and R. A. Walton, *Inorg. Chem.*, **14**, 1987 (1975).
(14) F. A. Cotton, B. A. Frenz, G. Deganello, and A. Shaver, *J. Organomet. Chem.*, **50**, 227 (1973).
(15) Computer programs used in data reduction and in solution and refinement of the structure were the following: DATARED by Frenz was used for

data reduction; absorption corrections were performed using the numerical subroutines of Coppens' DATAPP as included in AGNOST by Cohen; FOURIER, a version of Zalkin's FORDAP, by Dellaca and Robinson was used for Patterson and Fourier syntheses; the full-matrix, least-squares program NUCLS by Ibers and Doedens resembles Busing and Levy's ORFLS program; PERFACT by Frenz was used for an analysis of structure factors and ORTEP by Johnson was used for drawing illustrations on a Gerber plotter; the function and error program ORFFE by Busing, Martin, and Levy, as modified by Brown, Johnson, and Thiessen, was used; LIST by Snyder produced a listing of the data.
(16) D. T. Cromer and J. T. Waber, "International Tables for X-Ray Crystallography", Vol. IV, Kynoch Press, Birmingham, England, in press.
(17) D. T. Cromer and D. Liberman, *J. Chem. Phys.*, **53**, 1891 (1970).
(18) J. V. Brencic and F. A. Cotton, *Inorg. Chem.*, **8**, 7 (1969).
(19) F. A. Cotton, B. A. Frenz, B. R. Stults, and T. R. Webb, *J. Am. Chem. Soc.*, **98**, 2768 (1976).
(20) F. A. Cotton and E. Pedersen, *J. Am. Chem. Soc.*, **97**, 303 (1975); *Inorg. Chem.*, **14**, 383, 388, 399 (1975).
(21) F. A. Cotton, B. A. Frenz, E. Pedersen, and T. R. Webb, *Inorg. Chem.*, **14**, 391 (1975).
(22) F. A. Cotton and B. M. Foxman, *Inorg. Chem.*, **7**, 2135 (1968).
(23) M. J. Bennett, F. A. Cotton, and R. A. Walton, *Proc. R. Soc. London, Ser. A*, **303**, 175 (1968).
(24) The possibility that 3d orbitals of phosphorus or chlorine, or both, might furnish a suitable molecular orbital has been considered but rejected, since the interatomic overlaps of ligand d orbitals would probably be too small to generate a stable molecular orbital.

Synthesis, Structure, and Magnetism of Polynuclear Chelates. Structural and Magnetic Comparison of In-Plane and Out-of-Plane Exchange in Three Polynuclear Copper Complexes

R. L. LINTVEDT,* M. D. GLICK,* B. K. TOMLONOVIC, D. P. GAVEL, and J. M. KUSZAJ

Three related Cu(II) complexes were prepared from 1,3,5-triketonate-type ligands and their structures determined by single-crystal x-ray techniques. The complexes are $Cu_2(BAA)_2(py)_2$, containing the ligand 1-phenyl-1,3,5-hexanetrionate dianion, $[Cu_2(DTFACP)_2(H_2O)_2]_2$, containing the dianion of 2,5-bis(trifluoroacetyl)cyclopentanone, and $[CuH_2(BAA)_2en]_2$, containing the dianion of N,N'-bis(benzoylacetylacetone)ethylenediamine. The results show that $Cu_2(BAA)_2(py)_2$ is a binuclear monomer with each of the two copper atoms coordinated to four equatorial ketonic oxygens and one pyridine in typical five-coordinate manner: $Pbca$, $a = 8.473$ (3) Å, $b = 25.377$ (15) Å, $c = 19.000$ (10) Å, $Z = 4$, $R = 0.061$. The complex $[Cu_2(DTFACP)_2(H_2O)_2]_2$ is a dimer of binuclear molecules in which each copper atom is bonded to four equatorial ketonic oxygens and one axial H_2O (2.31 Å): $Pbca$, $a = 10.721$ (10) Å, $b = 24.634$ (10) Å, $c = 17.739$ (16) Å, $Z = 8$, $R = 0.066$. The complex $[CuH_2(BAA)_2en]_2$ is a mononuclear dimer in which the copper atom is bonded to four equatorial ketonic oxygens and an axial oxygen from the adjacent molecule (2.60 Å): $P2_1/c$, $a = 10.745$ (2) Å, $b = 9.205$ (2) Å, $c = 23.388$ Å, $\beta = 100.04$ (2)°, $Z = 4$, $R = 0.056$. The magnetic exchange pathways possible in the complexes are as follows: $Cu_2(BAA)_2(py)_2$, in-plane exchange; $[Cu_2(DTFACP)_2(H_2O)_2]_2$, both in-plane and out-of-plane exchange; $[CuH_2(BAA)_2en]_2$, out-of-plane exchange. The similarities between the magnetic properties of $Cu_2(BAA)_2(py)_2$ and $[Cu_2(DTFACP)_2(H_2O)_2]_2$ suggest only negligible out-of-plane exchange in the latter compound. Both of these compounds exhibit strong antiferromagnetism with exchange constants, J, of about -370 cm^{-1}. The validity of ignoring the out-of-plane exchange is supported by the normal magnetic behavior of $[CuH_2(BAA)_2en]_2$ down to 10 K.

Introduction

The β-polyketonates are an interesting and versatile class of ligands, especially when considered as a homologous series in which the 1,3-diketonates are the simplest members. In all probability, the higher homologues have coordinating ability similar to that of the 1,3-diketonates with the added dimension of being able to chelate more than one metal ion within the same molecule. The subject of a continuing program in our laboratory is the structure and magnetic superexchange in multinuclear chelates of β-polyketonates. These ligands offer a singularly attractive opportunity to investigate superexchange between several different metal ions in very similar ligand environments. Under such conditions, magnetic exchange is largely determined by the symmetry of the exchanging

electrons which in turn is determined by the ligand field symmetry. Our immediate goals are (1) to characterize the magnetic properties of the possible binuclear complexes with electronic configurations d^1–d^1 through d^9–d^9 and (2) to gather enough structural data to allow a general discussion of structural characteristics as they pertain to magnetic exchange. To date, the studies have included structural and magnetic results on 1,3,5-triketonates and their Schiff base derivatives: d^7–d^7 (Co^{2+}–Co^{2+}),[1] d^8–d^8 (Ni^{2+}–Ni^{2+}),[2] d^9–d^9 (Cu^{2+}–Cu^{2+}),[3] d^8–d^{10} (Ni^{2+}–Zn^{2+}),[4] and d^8–d^1 (Ni^{2+}–VO^{2+}).[5] In addition, magnetic studies have been carried out on d^1–d^1 (VO^{2+}–VO^{2+})[6] and d^3–d^3 (Cr^{3+}–Cr^{3+})[7] complexes. Many of the structural and magnetic data have been reviewed by Glick and Lintvedt.[7] The present work is concerned with the

structure and magnetism of three related Cu(II) complexes of either 1,3,5-triketonates or an ethylenediamine–Schiff base derivative: a mononuclear dimer, a binuclear monomer, and a binuclear dimer. Certain structural features presumed to be important in magnetic exchange mechanisms are well defined and relatively simple in these compounds.

In discussions of magnetic exchange between metals bridged by a diamagnetic atom (or atoms), the bridging angle is most often considered to be the determining factor in the exchange mechanism. In simple systems, such as d^9–d^9 exchange, the limiting values of 90 and 180° are presumed to result in ferro- and antiferromagnetic exchange, respectively. The theoretical explanation for the different mechanisms is based on the presence of an orthogonality plane for 90° and the absence of such a plane for 180°.[8] However, two other structural features which should be considered when correlating structural and magnetic data for polynuclear complexes are the orientation of the interacting magnetic planes and the dihedral angle between these planes. If one defines the magnetic plane in Cu(II) complexes as the plane of the orbital or orbitals containing the unpaired electron, then in the compounds discussed below, one contains parallel planes, a second coplanar planes, and the third a combination of both parallel and coplanar planes.

Experimental Section

Synthesis of Ligands and Chelates. Benzoylacetylacetone, H₂BAA. The β-triketone 1-phenyl-1,3,5-hexanetrione whose trivial name is benzoylacetylacetone was prepared by the method of Miles, Harris, and Hauser.[9] This method involves condensation of 2,4-pentanedione and ethyl benzoate in refluxing 1,2-dimethoxyethane with NaH as the base. The product is produced in quite high yields.

Bis(benzoylacetylacetonato)bispyridinedicopper(II), Cu₂-(BAA)₂(py)₂. The nonadducted chelate Cu₂(BAA)₂ was prepared as reported by Murtha and Lintvedt.[10] The pyridine derivative was prepared by dissolving Cu₂(BAA)₂ in pyridine and allowing this solution to evaporate to dryness in a hood. The reddish brown product was then redissolved in pyridine and this solution was allowed to evaporate slowly at room temperature. Crystals suitable for structure determination were obtained from this solution. The reddish brown crystals were collected on a sintered-glass filter and air-dried on the filter for 3–4 h. During drying, the crystals crumble presumably due to the loss of pyridines of crystallization. For this reason, crystals used in the structure determination must not be air-dried and, indeed, must be stored in a pyridine atmosphere. Anal. Calcd for Cu₂-(C₁₂H₁₀O₃)₂(C₅H₅N)₂: C, 59.22; H, 4.35; N, 4.06. Found: C, 58.89; H, 4.54; N, 4.04.

N,N'-Bis(benzoylacetylacetone)ethylenediamine, H₄(BAA)₂en. This ethylenediamine–Schiff base derivative was prepared by adding 1.0 ml (0.90 g, 0.015 mol) of ethylenediamine dropwise to a hot solution of 6.09 g (0.03 mol) of benzoylacetylacetone in 200 ml of absolute methanol. After a short period of heating and stirring a canary yellow precipitate formed. Heating was continued until the volume was reduced to about 100 ml after which the mixture was cooled to 0 °C and filtered. The product was recrystallized from acetone and air-dried. The yield was in excess of 90%. The bright yellow product melted at 171 °C. Anal. Calcd for C₂₆H₂₈N₂O₄: C, 72.19; H, 6.52; N, 6.45. Found: C, 71.84; H, 6.45; N, 6.66.

[N,N'-Bis(benzoylacetylacetonato)ethylenediamine]copper(II), CuH₂(BAA)₂en. Equimolar amounts of H₄(BAA)₂en and Cu(C-H₃COO)₂·H₂O were dissolved in an excess of acetone and a minimum of water, respectively, the volume of the aqueous Cu(II) solution being less than 10% of ligand acetone solution volume. The Cu(II) solution was then added slowly to boiling ligand solution. Chelation occurred immediately and precipitation began after the addition of a small fraction of the Cu(II) solution. After precipitation was complete, the mixture was filtered, and the product was washed with cold acetone and methanol and air-dried. Yields were typically greater than 80%. The product may be recrystallized from acetone yielding green-brown crystals which melt in a 2–3 °C range at 228 °C. Anal. Calcd for Cu(C₂₆H₂₆N₂O₄): C, 63.19; H, 5.30; N, 5.65; Cu, 12.90. Found: C, 63.01; H, 5.38; N, 5.54; Cu, 12.72.

Bis[2,5-bis(trifluoroacetyl)cyclopentanato]diaquodicopper(II) Hydrate, Cu₂(DTFACP)₂(H₂O)₂·H₂O. The protonated ligand was

not isolated, but rather the chelate was prepared directly from the sodium salt of the ligand. The sodium salt was prepared by the following method. Six-tenths mole of NaH and 100 ml of 1,2-dimethoxyethane were added to a 1000-ml, three-necked flask fitted with a reflux condenser, mechanical stirrer, and a dropping funnel. A solution of 0.1 mol of dry cyclopentanone and 0.2 mol of ethyl trifluoroacetate in 100 ml of 1,2-dimethoxyethane was placed in the dropping funnel and added slowly to the NaH under refluxing conditions. The entire mixture was refluxed for 12 h after which the solvent was removed by aspiration. To the dry solid was added 100 ml of diethyl ether, the slurry was cooled, and water was carefully added 1 drop at a time until the excess NaH had reacted. The solid product was collected on a sintered-glass filter, washed with diethyl ether, and air-dried. The sodium salt of the ligand, 6.4 g (ca. 0.02 mol), was dissolved in 150 ml of methanol, and in a separate beaker 9.66 g (0.04 mol) of Cu(NO₃)₂·3H₂O was dissolved in 100 ml of methanol. The two solutions were combined and the mixture was refluxed for 12 h, after which the volume was decreased to about 75 ml and 100 ml of water was added. The resulting solid was filtered and air-dried. The crude product may be recrystallized from methanol, 1,2-dimethoxyethane, or CHCl₃. The last solvent produced crystals suitable for structure determination. Anal. Calcd for Cu₂-(C₉H₄F₆O₃)₂(H₂O)₂·H₂O: C, 29.47; H, 2.46; Cu, 17.33. Found: C, 29.83; H, 2.44; Cu, 17.49.

Magnetic Susceptibility. Magnetic susceptibility as a function of temperature was measured using the standard Faraday technique, with Hg[Co(SCN)₄] as the calibrant.[11] Temperature measurements were made using a copper–constantan thermocouple connected to a Leeds and Northrup temperature potentiometer, yielding an accuracy of ±0.5 K. The measurements were taken using a Varian Associates Model V-4004 4-in. electromagnet with a 2-in. pole gap. The resulting fields are about 8000 G. Measurements recorded below 77 K were obtained using a zero-field induction bridge method and the same calibrant. In all cases, corrections for diamagnetism were made using Pascal's constants.

Structure Determinations. Cu₂(DTFACP)₂(H₂O)₂·H₂O. A crystal of truncated octahedral geometry with a maximum dimension of about 0.3 mm was mounted on a glass fiber with Silastic adhesive. Precession photographs (Cu Kα) were uniquely consistent with the orthohomic space group *Pbca*. Final lattice constants were obtained from a least-squares refinement[12] of 20 reflections centered on a Picker four-circle card-controlled diffractometer with Mo Kα₁ radiation (λ 0.709 26 Å). The unit cell data are $a = 10.721$ (10) Å, $b = 24.634$ (10) Å, $c = 17.739$ (16) Å, ρ(calcd) = 2.08 g/cm³, ρ(flotation) = 2.09 (3) g/cm³, $Z = 8$ binuclear molecules, and $\mu = 20.48$ cm⁻¹.

Intensity data were collected with Nb-filtered Mo Kα radiation by the θ–2θ scan technique with a takeoff angle of 2.7°, a symmetric scan of 2.0° (minimum) with an allowance for spectral dispersion, and a scan rate of 2°/min. Background counts were taken at each end of the scan for 15 s. Copper attenuators were inserted for reflections which exceeded 9000 counts/s. The intensities of four standard reflections monitored every 100 data fluctuated less than 3.5%.

Standard deviations were assigned as

$$\sigma(I) = [P + (B_1 + B_2)\Delta(2\theta) + (0.05I)^2]^{1/2}$$

where P is the gross intensity, B_1 and B_2 are the background counts, $\Delta(2\theta)$ is the scan width, and I is the net intensity. Of the 4185 data examined with $(\sin \theta)/\lambda < 0.595$, 2604 had $F^2 > 2.5\sigma(F^2)$ and were used for solution and refinement with weights equal to $\sigma(F)^{-2}$.

The asymmetric unit comprises one binuclear molecule. Analysis of a three-dimensional Patterson synthesis yielded the positions of the two independent copper atoms. Subsequent three-dimensional Fourier syntheses allowed the positioning of the remaining nonhydrogen atoms. Full-matrix, least-squares refinement with isotropic models for carbon and oxygen atoms and anisotropic models for copper and fluorine atoms yielded an unweighted discrepancy factor $R = \sum(\|F_o\| - |F_c\|)/\sum|F_o| = 0.085$ and a weighted discrepancy factor $R_w = \{\sum w(|F_o| - |F_c|)^2/\sum wF_o^2\}^{1/2} = 0.103$.

Ten of the fourteen hydrogen atoms were located on a difference Fourier map. Refinement with all nonhydrogen atoms assigned anisotropic thermal parameters, fixed contributions from the located hydrogen atoms, and, including anomalous scattering effects for the copper atoms, yielded $R = 0.066$, $R_w = 0.073$, and an error of fit of 2.11. The highest residual electron density was 0.90 e/Å³ near the metal positions. A listing of observed and calculated structure factors

Table I. Atomic Parameters for $Cu_2(DTFACP)_2(H_2O)_2 \cdot H_2O^a$

	x	y	z		x	y	z
Cu1	0.0203 (1)	0.0171 (0)	0.1550 (1)	C13	-0.1618 (9)	-0.1072 (3)	0.0402 (5)
Cu2	-0.1640 (1)	0.0239 (0)	0.0285 (1)	C14	-0.0731 (9)	-0.0797 (3)	0.0845 (5)
O1	-0.2377 (6)	0.0858 (2)	-0.0195 (3)	C15	-0.2346 (9)	-0.0826 (4)	-0.0133 (5)
O2	-0.0585 (5)	0.0578 (2)	0.0912 (3)	C16	-0.3380 (12)	-0.1134 (4)	-0.0525 (7)
O3	0.1083 (6)	0.0729 (3)	0.2118 (4)	C17	0.1523 (16)	0.1568 (5)	0.2616 (8)
O4	0.1112 (6)	-0.0440 (2)	0.1969 (4)	C18	0.1299 (13)	-0.1310 (5)	0.2459 (7)
O5	-0.0502 (5)	-0.0279 (2)	0.0769 (3)	O8	-0.1334 (7)	0.0078 (3)	0.2381 (4)
O6	-0.2317 (6)	-0.0317 (2)	-0.0340 (3)	O9	-0.0720 (7)	-0.0264 (3)	0.3869 (4)
O7	-0.3195 (7)	0.0122 (3)	0.1177 (4)	F1	-0.3789 (6)	0.1996 (2)	0.0089 (4)
C1	-0.2993 (9)	0.1757 (4)	-0.0389 (6)	F2	-0.3713 (6)	0.1533 (3)	-0.0923 (4)
C2	-0.2165 (8)	0.1360 (4)	0.0006 (5)	F3	-0.2373 (6)	0.2158 (2)	-0.0713 (4)
C3	-0.1335 (8)	0.1549 (4)	0.0532 (5)	F4	-0.4423 (7)	-0.1063 (5)	-0.0192 (6)
C4	-0.1142 (10)	0.2132 (4)	0.0787 (6)	F5	-0.3202 (8)	-0.1642 (3)	-0.0599 (6)
C5	-0.0155 (10)	0.2095 (4)	0.1418 (6)	F6	-0.3570 (8)	-0.0960 (3)	-0.1219 (5)
C6	0.0119 (8)	0.1492 (4)	0.1514 (5)	F7	0.2081 (10)	0.1992 (4)	0.2371 (5)
C7	-0.0589 (8)	0.1205 (3)	0.0974 (5)	F8	0.2275 (13)	0.1330 (4)	0.3011 (8)
C8	0.0867 (9)	0.1239 (4)	0.2041 (5)	F9	0.0762 (12)	0.1799 (6)	0.3083 (6)
C9	0.0717 (9)	-0.0929 (4)	0.1887 (5)	F10	0.0730 (15)	-0.1310 (6)	0.3060 (5)
C10	-0.0122 (9)	-0.1131 (3)	0.1373 (5)	F11	0.2423 (11)	-0.1188 (4)	0.2605 (8)
C11	-0.0622 (10)	-0.1707 (4)	0.1278 (6)	F12	0.1387 (12)	-0.1803 (3)	0.2289 (5)
C12	-0.1649 (10)	-0.1664 (4)	0.0548 (6)				

	β_{11}	β_{22}	β_{33}	β_{12}	β_{13}	β_{23}
Cu1	0.0073 (1)	0.0008 (1)	0.0028 (1)	-0.0000 (1)	-0.0014 (1)	0.0001 (1)
Cu2	0.0068 (1)	0.0007 (1)	0.0025 (1)	-0.0001 (1)	-0.0011 (1)	0.0000 (1)
O1	0.0073 (7)	0.0009 (1)	0.0027 (2)	0.0001 (2)	-0.0012 (3)	0.0002 (1)
O2	0.0053 (6)	0.0008 (1)	0.0025 (2)	-0.0003 (2)	-0.0010 (3)	0.0002 (1)
O3	0.0096 (8)	0.0012 (1)	0.0036 (3)	-0.0007 (3)	-0.0028 (4)	-0.0001 (2)
O4	0.0098 (8)	0.0009 (1)	0.0033 (2)	0.0001 (2)	-0.0014 (4)	0.0002 (1)
O5	0.0073 (7)	0.0006 (1)	0.0023 (2)	-0.0004 (2)	-0.0006 (3)	0.0002 (1)
O6	0.0090 (7)	0.0008 (1)	0.0033 (2)	-0.0005 (2)	-0.0013 (4)	0.0000 (1)
O7	0.0089 (8)	0.0031 (2)	0.0037 (3)	-0.0013 (3)	-0.0007 (4)	0.0003 (2)
C1	0.0082 (11)	0.0010 (2)	0.0033 (4)	-0.0002 (4)	-0.0007 (5)	0.0006 (2)
C2	0.0054 (9)	0.0009 (2)	0.0025 (3)	0.0004 (3)	0.0002 (4)	0.0001 (2)
C3	0.0051 (9)	0.0009 (2)	0.0027 (3)	-0.0000 (3)	-0.0001 (4)	0.0002 (2)
C4	0.0124 (12)	0.0007 (2)	0.0034 (4)	-0.0002 (4)	-0.0011 (6)	0.0001 (2)
C5	0.0126 (13)	0.0009 (2)	0.0038 (4)	-0.0003 (4)	-0.0025 (6)	-0.0002 (2)
C6	0.0053 (9)	0.0010 (2)	0.0025 (3)	-0.0005 (3)	0.0003 (5)	-0.0001 (2)
C7	0.0040 (8)	0.0009 (2)	0.0023 (3)	-0.0000 (3)	0.0002 (4)	0.0003 (2)
C8	0.0080 (11)	0.0009 (2)	0.0029 (4)	-0.0006 (3)	-0.0009 (5)	-0.0001 (2)
C9	0.0055 (9)	0.0013 (2)	0.0027 (3)	0.0007 (3)	0.0001 (5)	0.0004 (2)
C10	0.0073 (10)	0.0007 (1)	0.0030 (4)	0.0003 (3)	0.0012 (5)	0.0003 (2)
C11	0.0099 (12)	0.0008 (2)	0.0034 (4)	0.0000 (3)	0.0002 (6)	0.0002 (2)
C12	0.0130 (13)	0.0006 (2)	0.0037 (4)	0.0001 (4)	-0.0000 (7)	-0.0002 (2)
C13	0.0059 (9)	0.0009 (2)	0.0030 (4)	-0.0002 (3)	0.0002 (5)	-0.0003 (2)
C14	0.0064 (9)	0.0008 (2)	0.0027 (4)	0.0002 (3)	0.0007 (5)	-0.0000 (2)
C15	0.0061 (9)	0.0012 (2)	0.0024 (3)	-0.0002 (3)	-0.0001 (5)	-0.0003 (2)
C16	0.0106 (14)	0.0014 (2)	0.0040 (5)	-0.0012 (5)	-0.0002 (7)	-0.0004 (2)
C18	0.0191 (19)	0.0014 (2)	0.0040 (5)	-0.0009 (6)	-0.0033 (9)	-0.0004 (3)
C19	0.0131 (16)	0.0016 (2)	0.0038 (5)	0.0012 (5)	-0.0012 (7)	0.0006 (3)
O8	0.0103 (8)	0.0033 (2)	0.0027 (3)	-0.0010 (3)	0.0006 (4)	-0.0000 (2)
O9	0.0096 (8)	0.0021 (2)	0.0040 (3)	0.0000 (3)	0.0019 (4)	0.0005 (2)
F1	0.0105 (7)	0.0021 (1)	0.0056 (3)	0.0020 (3)	-0.0002 (4)	0.0002 (2)
F2	0.0157 (9)	0.0020 (1)	0.0049 (3)	0.0006 (3)	-0.0047 (5)	0.0004 (2)
F3	0.0122 (8)	0.0021 (1)	0.0059 (3)	0.0002 (3)	-0.0003 (4)	0.0022 (2)
F4	0.0105 (9)	0.0085 (4)	0.0115 (6)	-0.0058 (5)	0.0041 (6)	-0.0057 (4)
F5	0.0271 (14)	0.0014 (1)	0.0133 (6)	-0.0005 (4)	-0.0119 (8)	-0.0016 (2)
F6	0.0249 (15)	0.0034 (2)	0.0060 (4)	-0.0045 (4)	-0.0064 (6)	0.0002 (2)
F7	0.0383 (19)	0.0041 (2)	0.0078 (5)	-0.0086 (6)	-0.0072 (8)	0.0002 (3)
F8	0.0548 (29)	0.0027 (2)	0.0172 (9)	0.0025 (6)	-0.0275 (15)	-0.0024 (4)
F9	0.0296 (19)	0.0088 (5)	0.0075 (5)	-0.0017 (8)	-0.0015 (8)	-0.0055 (4)
F10	0.0515 (30)	0.0111 (6)	0.0052 (4)	0.0177 (11)	0.0070 (9)	0.0054 (4)
F11	0.0250 (15)	0.0044 (3)	0.0203 (11)	-0.0027 (6)	-0.0152 (12)	0.0063 (5)
F12	0.0491 (22)	0.0018 (2)	0.0085 (5)	0.0044 (5)	-0.0106 (9)	0.0004 (2)

a Standard deviations from the full variance–covariance matrix are given in parentheses for the least significant digit(s). The form of the anisotropic temperature factor is $\exp[-(h^2\beta_{11} + k^2\beta_{22} + l^2\beta_{33} + 2hk\beta_{12} + 2hl\beta_{13} + kl\beta_{23})]$. The hydrogen atoms were added as fixed contributions and assigned an isotropic temperature factor of 6.0.

is available.[13] Table I contains a listing of atomic coordinates and anisotropic thermal parameters.

[CuH₂(BAA)₂en]₂. A single crystal in the form of a rectangular parallelepiped with dimensions of 0.25 × 0.26 × 0.09 mm was mounted on a glass fiber with epoxy adhesive. Precession photographs were uniquely consistent with the monoclinic space group $P2_1/c$. Lattice constants were obtained from least-squares refinement of 15 reflections centered on a Syntex $P2_1$ diffractometer with Mo Kα radiation (λ 0.710 69 Å) which had been diffracted from a highly oriented graphite crystal whose diffraction vector was parallel to that of the crystal. The unit cell parameters are a = 10.745 (2) Å, b = 9.205 (2) Å, c = 23.388 (5) Å, β = 100.04 (2)°, ρ(calcd) = 1.44 g/cm³, ρ(flotation) = 1.43 g/cm³, Z = 4 molecules, and μ = 10.34 cm⁻¹.

Intensity data to $(\sin \theta)/\lambda < 0.595$ were collected with Mo Kα

radiation on the Syntex diffractometer by the θ–2θ technique. The scan rate was inversely proportional to the peak intensity and ranged between 0.93 and 3.99°/min. The scan range was 2θ(Mo Kα_1) – 0.8° to 2θ(Mo Kα_2) + 0.9°. Backgrounds were measured at each end of the scan for a total time equal to half the scan time. The intensities of five standard reflections measured following every 100 data showed no significant fluctuation.

Standard deviations for data collected on the Syntex diffractometer were assigned as

$$\sigma(I) = [\sigma_{\text{counter}}(I)^2 + (pI)^2]^{1/2}$$

where $\sigma_{\text{counter}} = (I + K^2B)^{1/2}$, I is the net intensity, B is the total background counts, K is the ratio of scan time to background time, and p is an instability factor equal to 0.05. Of the 4553 independent data examined, 2694 had $F^2 > 3\sigma(F^2)$ and were used in the solution and refinement process.

Analysis of a three-dimensional Patterson synthesis yielded the position of the independent copper atom. Subsequent three-dimensional Fourier maps contained the positions of all the nonhydrogen atoms. Full-matrix, least-squares refinement of all of the nonhydrogen atom coordinates with isotropic thermal parameters resulted in $R = 0.096$ and $R_w = 0.115$. At this point all hydrogen atoms except those attached to the nitrogens were located from a difference Fourier map. Refinement in two blocks with isotropic thermal parameters for hydrogen atoms and anisotropic thermal parameters for all other atoms yielded $R = 0.056$, $R_w = 0.062$, and an error of fit of 1.40. The largest nonmetal residual was 0.56 e/Å^3. Table II contains a listing of atomic coordinates and thermal parameters. A listing of calculated and observed structure factors is available.[13]

Cu$_2$(BAA)$_2$(py)$_2$·2py. Since the thin red plates decomposed to a red-brown powder after several minutes' exposure to air, it was necessary to mount the crystal in a capillary tube containing a small amount of the mother liquor to prevent decomposition and a touch of grease to increase adherence to the wall. In spite of these precautions the crystal tended to move in the capillary and to decompose, such that it was necessary to use a high rate of data collection in order to attain a full set of data.

A preliminary x-ray study of this compound was carried out with a very small crystal. Rotation photographs and intensity data from this crystal established the orthorhombic space group *Pbca*. A total of 1949 independent data with (sin θ)/λ < 0.42 were examined as described for the immediately preceding compound at a scan rate of 4°/min. Of these, 476 data had $F^2 > 3\sigma(F^2)$ which were used in the solution.

The space group requires the location of half of a Cu$_2$(BAA)$_2$-(py)$_2$·2py unit. A Patterson synthesis yielded the location of the independent copper atom. Although the resulting Fourier map phased on this position contained pseudosymmetry, it was possible, by proceeding stepwise, to extract the positions of all nonhydrogen atoms from a series of Fourier syntheses. Isotropic least-squares refinement yielded $R = 0.063$ and $R_w = 0.067$. This refinement required the fitting of 113 parameters to 467 data; even the use of rigid-body refinement left an inadequate data:parameter ratio.

A higher quality crystal with dimensions 0.45 × 0.30 × 0.11 mm was found after the examination and rejection of a number of unsatisfactory crystals. Least-squares refinement of 15 reflections accurately centered with Mo Kα radiation on the Syntex *P*2$_1$ diffractometer yielded unit cell parameters of $a = 8.473$ (3) Å, $b = 25.377$ (15) Å, $c = 19.000$ (10) Å, and ρ(calcd) = 1.379 g/cm^3 for 4 formula units of Cu$_2$(C$_{24}$H$_{20}$O$_2$)(C$_5$H$_5$N)$_2$·2C$_5$H$_5$N. Intensity data to a value of (sin θ)/λ < 0.50 were collected at a scan rate of 4°/min with a scan varying in 2θ width between 1.5 and 2.2°; backgrounds were counted at the ends of the scans for a time equal to half of the scan time. Even with this crystal, it was necessary to recenter periodically as the crystal continued to move in the mother liquor; the need to recenter was dictated by the intensity of the [$\bar{1}$11] reflection.

Of the 2580 data examined, 950 had $F^2 > 3\sigma(F^2)$ (with $\sigma(F^2)$ defined as above and an instability factor of 0.03) and were used in the final refinement. Isotropic full-matrix least-squares refinement for all nonhydrogen atoms converged with $R = 0.066$ and $R_w = 0.071$. Refinement with anisotropic thermal parameters for the copper and oxygen atoms reduced the discrepancy factors to $R = 0.061$ and $R_w = 0.067$ with an error of fit of 2.46. Table III contains a listing of atomic coordinates and thermal parameters. A listing of calculated and observed structure factors is available.[13] Table IV contains atomic

displacements from the relevant mean plane of each of the structures studied.

Results

Magnetic Data. [CuH$_2$(BAA)$_2$en]$_2$. The magnetic susceptibility for this oxygen-bridged dimer has been determined between room temperature and 4.5 K. Throughout this temperature range the susceptibility values may be characterized as normal. In other words, there is no detectable magnetic exchange between the Cu(II) ions down to about 7 K below which it appears as if antiferromagnetism is observed. The magnetic results are presented in Table V. The EPR spectra contain a half-field absorption (ca. 1500 G) which increases in intensity at low temperatures (10 K).

[Cu$_2$(DTFACP)$_2$(H$_2$O)$_2$]$_2$·2H$_2$O. The magnetic susceptibility in the temperature range 77–400 K is presented in Table VI. These susceptibility data have been corrected for temperature-independent paramagnetism ($N\alpha$) assuming a value of 100×10^{-6} cgsu/Cu(II). The magnetic susceptibility is very low throughout this temperature range indicating very strong antiferromagnetic exchange between the copper ions. The data have been corrected for 3% paramagnetic impurity in column 4 of Table VI for two reasons. (1) The usual treatment of strong antiferromagnetic exchange dictates that a compound with χ'_m as low as 200×10^{-6} cgsu at 297 K should have a χ'_m of zero well before 77 K. (2) The EPR spectrum consists of absorptions typical of an isolated single Cu(II) and persists down to 10 K, which is consistent with the presence of a small concentration of a mononuclear Cu(II) impurity. The value of 3% is somewhat arbitrary. It was chosen in order to give near-zero $\chi'_m - N\alpha$ values at the lower temperatures, in accord with the expected thermal population of spin states throughout the temperature range studied. The last column of Table VI contains susceptibilities calculated using the well-known Bleaney–Bowers equation[14] with $g = 2.12$ and $J = -370$ cm^{-1}. The agreement between χ'_m(cor) and χ'_m(calcd) is very good and certainly within experimental error.

The waters on this binuclear dimer are easily removed quantitatively in vacuo, as determined by gravimetric analysis using the same electrobalance that is used in conjunction with the Faraday susceptibility measurements. The loss of water is accompanied by the crystals crumbling into a powder. The magnetic properties of the new dimer, [Cu$_2$(DTFACP)$_2$]$_2$, are identical with those of the original, crystalline compound.

Cu$_2$(BAA)$_2$(py)$_2$. This molecule, which contains two coppers bridged by two oxygens and roughly in the same plane, has an extremely low susceptibility even at room temperature. At 300 K, $\chi'_m - N\alpha$ is 130×10^{-6} cgsu, and at 77 K, $\chi'_m - N\alpha$ is 70×10^{-6} cgsu assuming $N\alpha = 100 \times 10^{-6}$ cgsu. The low-temperature EPR spectrum indicates that a small amount of paramagnetic Cu(II) is present, presumably due to mononuclear impurities. If the measured values are corrected for about 1.5% paramagnetic Cu(II), the room-temperature moment becomes 0.5 μ_B and the compound is diamagnetic at 77 K. These results are very similar to those found for the tetranuclear [Cu$_2$(DTFACP)$_2$(H$_2$O)$_2$]$_2$, and, therefore, the exchange constants are very similar, as well.

Structural Data. [Cu$_2$(DTFACP)$_2$(H$_2$O)$_2$·H$_2$O]$_2$. This complex crystallizes as a dimer in which pairs of binuclear units related by inversion centers are weakly interacting. Figures 1 and 2 show the packing of the units in the cell and a single molecular unit. The molecular unit comprises two coppers coordinated to two of the triketonate ligands in a fashion similar to that of the previously reported triketonates. Each copper is strongly coordinated to four equatorial ketonic oxygens (1.9 Å average) and an axial water oxygen at 2.31 Å (average). The sixth coordination site is occupied by a ketonic oxygen of the symmetry-related molecule at a distance
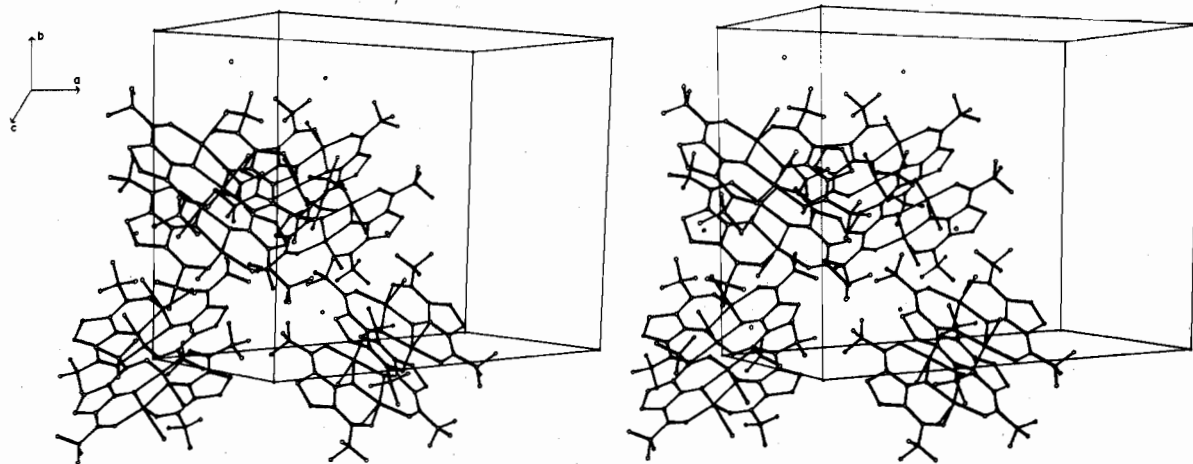
Figure 1. Packing diagram of $[Cu_2(DTFACP)_2(H_2O)_2 \cdot H_2O]_2$.
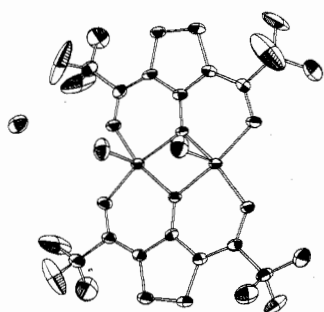
Figure 2. Molecular structure of $Cu_2(DTFACP)_2(H_2O)_2 \cdot H_2O$ with thermal ellipsoids.

of 3.01 Å (average). The only interaction between adjacent dimers is via hydrogen bonding with the uncoordinated waters of hydration. The labeling, distances, and angles are shown in Figures 3 and 4.

In Figure 5 is shown the coordination environment of the dimer. Each copper atom is displaced 0.10 Å (average) from the plane of the triketonate ligand toward the more strongly bound axial ligands, the water molecules. The ligand framework is relatively unaffected by the closure of the cyclopentano fragment. The coordination spheres of the coppers are distorted octahedra with normal basal oxygen–copper distances. The copper–oxygen distances to the bridging oxygens (O2 and O5) are slightly longer than the terminal oxygen–copper distances resulting from the additional bond formed by these oxygens. The Cu–O5 distance is slightly longer than the Cu–O2 distance which is probably due to the fact that O5 is also interacting intermolecularly with a copper from the adjacent molecule. The fifth coordination sites on each copper are occupied by the oxygens of water molecules (O7 and O8) at average distances of 2.314 Å. The two coordinated water molecules are on the same side of the plane described by the two coppers and two triketonates. The sixth coordination sites are completed by oxygens from an adjacent molecule, one a bridging oxygen (O5) and one a terminal oxygen (O6).

The angles in the copper coordination spheres do not differ significantly from other triketonate chelates.[1-3] The Cu–O–Cu bridging angle, which is of critical importance in magnetic superexchange discussions, averages 103.8°. The intermolecular Cu–O–Cu′ bridging angle averages 85.8°. The decrease from the expected 90° angle for Cu–O–Cu′ most probably is due to packing constraints.

Cu₂(BAA)₂(py)₂·2py. In its general features, the structure of $Cu_2(BAA)_2(py)_2$ is quite similar to that of previously reported binuclear 1,3,5-triketonates. The unit cell contains

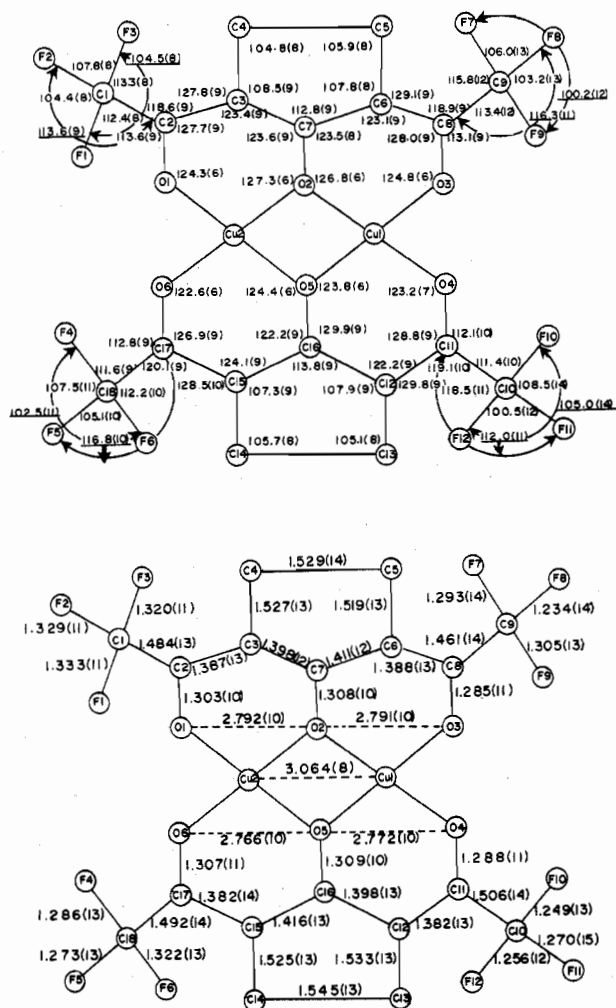**Figure 3.** Atomic labeling and intramolecular distances and angles (in Å and deg) in the ligand of $Cu_2(DTFACP)_2(H_2O)_2 \cdot H_2O$.

four centrosymmetric binuclear molecules with each of the two copper atoms coordinated to four ketonic oxygens and one nitrogen from a pyridine molecule. The coordinated pyridines are on opposite sides of the molecular plane as shown in Figure 6 precluding any dimerization as found in the previous compound. In addition, there are two uncoordinated pyridine molecules per chelate molecule as seen in Figure 7. The position of the nitrogen atoms in these pyridines is indeterminate.
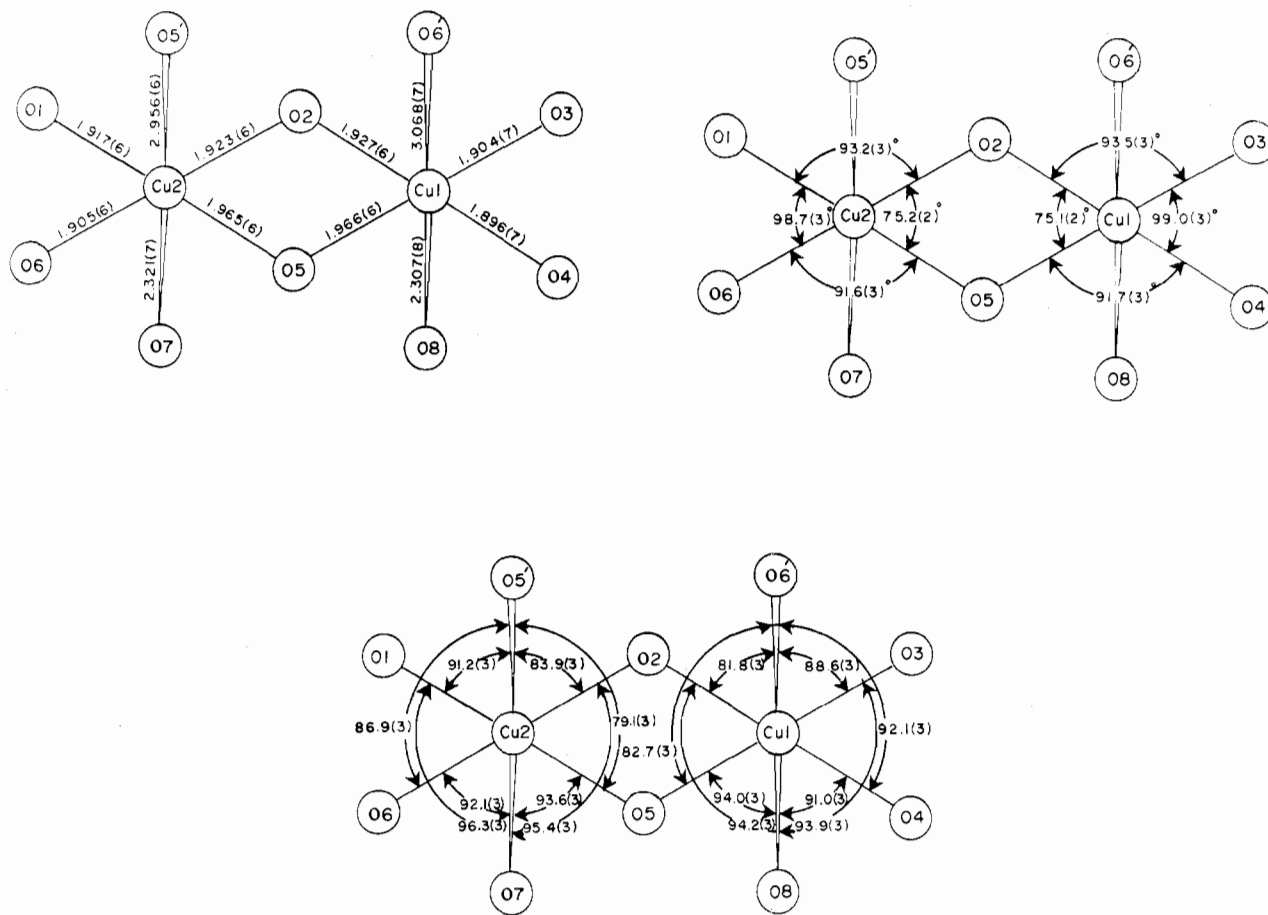
Figure 4. Distances and angles in the coordination sphere of $[Cu_2(DTFACP)_2(H_2O)_2 \cdot H_2O]_2$.
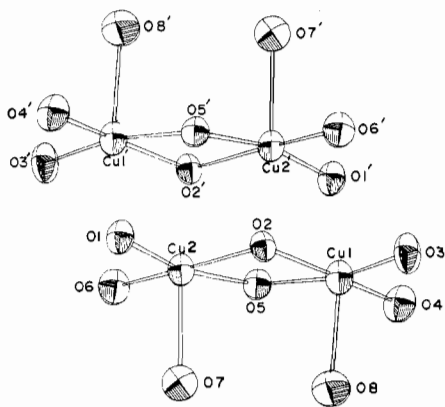

Figure 5. Coordination environment of the copper(II) ions in the binuclear dimer.

The pertinent bond distances and angles for this centrosymmetric molecule are shown in Figures 8 and 9. The bond distances and angles in the phenyl group and the pyridine rings are entirely as expected and warrant no additional comment here. The only nonhydrogen intermolecular distances less than 3.5 Å are between terminal oxygen atoms and carbon atoms of coordinated pyridines of adjacent molecules. These distances range from 3.25 to 3.42 Å and are presumed to have no chemical significance. Thus, these binuclear molecules are truly monomeric in the crystal, unlike the previous compound.

The parameters within the basal plane in $Cu_2(BAA)_2(py)_2$ are similar to those found in $Cu_2(DTFACP)_2(H_2O)_2$. The Cu–N distance of 2.274 Å is considerably shorter than the axial distances in $Cu_2(DTFACP)_2(H_2O)_2$ due to the partial localization of the antibonding electrons in the d_{z^2} orbital on

the side opposite the pyridine ligand in this five-coordinate system. The copper atom is displaced 0.23 Å toward the pyridine molecule in typical square-pyramidal fashion.
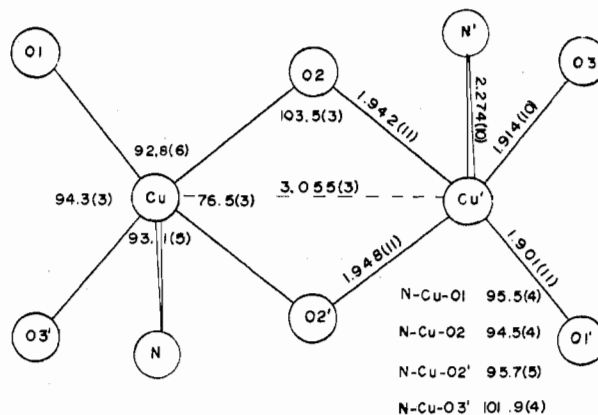
$[CuH_2(BAA)_2en]_2$. The molecular structure consists of one copper(II) ion coordinated to the dianionic Schiff base derivative of 1-phenyl-1,3,5-hexanetrione and ethylenediamine. The copper(II) ion is coordinated to the four ketonic oxygens leaving a second potential coordination site with two nitrogen and two oxygen donors vacant. One molecule and the atomic numbering scheme are shown in Figure 10. The single molecule is actually part of a dimeric unit as the fifth coordination position of the copper is occupied by the central oxygen of an adjacent molecule. One dimeric unit is shown in Figure 11. A stereoscopic view of the packing of these dimers in the unit cell is given in Figure 12. The pertinent bond angles, bond lengths, and nonbonded distances in the ligand are given in Figure 13.

Although the two remaining enolizable protons were not located in this study, the "backbone" C–C and C–N distances leave little doubt that hydrogens are associated with the nitrogens. Certainly the data in Figure 13 are consistent with sp^2 hybridization for C2 and C13 and not with sp^3 hybridization. Indeed, the distances and angles are almost identical with those in $Cu_2(BAA)_2(py)_2$ in which no enolizable protons remain. The distances and angles for the phenyl substituents are normal.

The angles and distances within the copper atom coordination sphere are shown in Figure 14. These appear to be normal in essentially all respects for five-coordinate copper-containing oxygen donors. The Cu–O2'–Cu' bond angle is 95.7° and the copper–copper distance is 3.38 Å, only 10% greater than the intramolecular copper–copper distance in $Cu_2(DTFACP)_2(H_2O)_2$ and $Cu_2(BAA)_2(py)_2$.
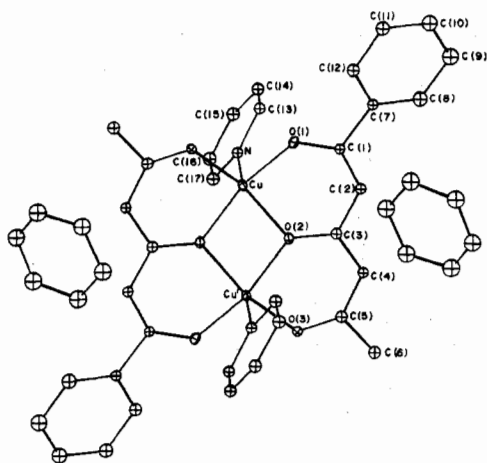
Figure 6. Molecular structure and atomic labeling of $Cu_2(BAA)_2(py)_2 \cdot 2py$.
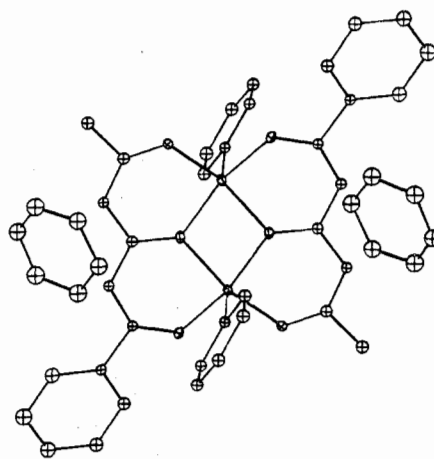
Figure 7. Packing diagram of $Cu_2(BAA)_2(py)_2 \cdot 2py$.
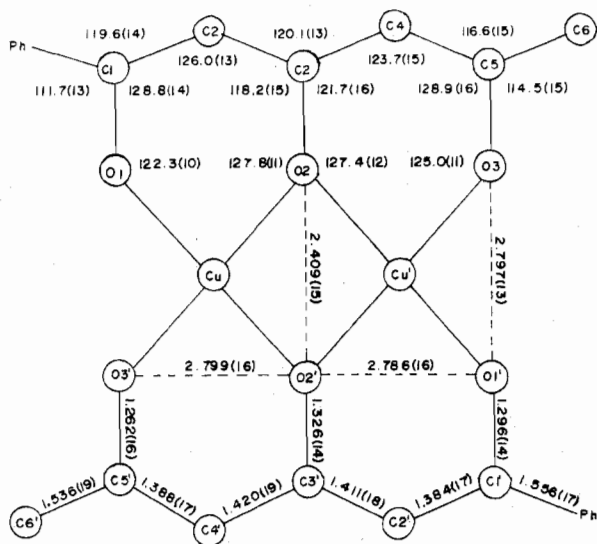
Figure 8. Distances and angles in the ligand of $Cu_2(BAA)_2$-$(py)_2 \cdot 2py$.

Figure 9. Distances and angles in the coordination sphere of Cu_2-$(BAA)_2(py)_2 \cdot 2py$.

However, in the absence of coordinated solvent, the axial interaction with the adjacent molecule is stronger than in the presence of the solvent molecule, since it is the primary rather than the secondary axial interaction.

Discussion

A fundamental reason for our continuing interest in β-polyketones and their derivatives as ligands for the preparation of polynuclear complexes is the likelihood that certain structural parameters important in magnetic exchange will be nearly invariant as one changes the metal ions. If this is in fact true, then differences in magnetic exchange in binuclear complexes between pairs of different metal ions should be a function of the symmetry of the exchanging electrons rather than any structural differences. It would, therefore, be possible to study d^1–d^1 through d^9–d^9 magnetic exchange in nearly constant environments. The structural data presently available

The equatorial geometry of the Cu(II) in $[CuH_2(BAA)_2en]_2$ is similar to those previously described in this study. The axial Cu–O distance of 2.603 Å to an adjacent molecule in this five-coordinate copper complex is longer than the distance to the strongly bound pyridine in the five-coordinate Cu_2-$(BAA)_2(py)_2$ and the distance to the strongly bound water in the six-coordinate $[Cu_2(DTFACP)_2(H_2O)_2 \cdot H_2O]_2$ but is shorter than the weak interaction to an adjacent molecule in the latter compound. Consistent with this is a small displacement (0.06 Å) of the copper toward the weakly bound axial oxygen. These distances and displacements clearly show that axial interactions with adjacent complex ions are weak compared with axial interactions with solvent molecules.

Table II. Atomic Parameters for [CuH₂(BAA)₂en]₂^a

	x	y	z		x	y	z
Cu	0.064 59 (6)	0.413 59 (8)	0.561 88 (3)	C23	0.5524 (7)	0.4992 (9)	0.7208 (3)
O1	0.229 1 (4)	0.414 5 (5)	0.607 1 (2)	C24	0.6520 (7)	0.3984 (11)	0.7274 (3)
O2	0.104 3 (4)	0.261 7 (4)	0.512 9 (2)	C25	0.6445 (7)	0.2774 (10)	0.6939 (3)
O3	−0.102 5 (3)	0.400 9 (5)	0.517 3 (2)	C26	0.5383 (6)	0.2538 (8)	0.6512 (3)
O4	0.011 1 (3)	0.548 6 (4)	0.614 2 (2)	H1	0.4068 (55)	0.1829 (66)	0.5585 (24)
N1	0.002 3 (5)	0.099 9 (6)	0.426 0 (2)	H2	0.2962 (54)	0.0452 (65)	0.4683 (24)
N2	−0.223 8 (5)	0.240 8 (6)	0.434 3 (2)	H3	0.2163 (57)	−0.1128 (67)	0.3998 (26)
C1	0.323 2 (5)	0.332 4 (7)	0.598 3 (2)	H4	0.1288 (56)	−0.0471 (67)	0.3596 (25)
C2	0.320 9 (5)	0.235 9 (7)	0.553 0 (3)	H5	0.0571 (56)	−0.1588 (68)	0.3908 (25)
C3	0.212 7 (6)	0.200 0 (6)	0.511 8 (2)	H6	−0.1579 (54)	−0.0342 (54)	0.4055 (25)
C4	0.216 8 (6)	0.088 8 (7)	0.469 9 (2)	H7	−0.0892 (56)	0.0056 (69)	0.3503 (25)
C5	0.115 0 (6)	0.040 0 (6)	0.430 3 (2)	H8	−0.2941 (55)	0.1176 (65)	0.3695 (24)
C6	0.132 1 (7)	−0.083 6 (8)	0.390 2 (3)	H9	−0.1755 (54)	0.2454 (68)	0.3529 (26)
C7	−0.111 6 (7)	0.051 5 (7)	0.388 8 (3)	H10	−0.4487 (56)	0.1095 (68)	0.4222 (24)
C8	−0.213 4 (6)	0.165 7 (8)	0.380 6 (3)	H11	−0.4669 (55)	0.2388 (70)	0.3916 (25)
C9	−0.450 2 (6)	0.205 5 (8)	0.430 3 (3)	H12	−0.5287 (54)	0.2288 (69)	0.4522 (25)
C10	−0.326 8 (5)	0.270 7 (7)	0.457 4 (3)	H13	−0.3915 (54)	0.3693 (66)	0.5223 (24)
C11	−0.318 6 (5)	0.358 6 (7)	0.505 0 (3)	H14	−0.2873 (53)	0.5281 (67)	0.6006 (24)
C12	−0.207 1 (5)	0.421 8 (7)	0.536 4 (2)	H15	−0.2940 (53)	0.7243 (67)	0.6435 (25)
C13	−0.209 0 (5)	0.504 6 (7)	0.587 2 (2)	H16	−0.3184 (54)	0.8622 (62)	0.7072 (24)
C14	−0.105 2 (5)	0.570 1 (7)	0.620 6 (2)	H17	−0.1533 (53)	0.9008 (62)	0.7977 (24)
C15	−0.123 2 (5)	0.667 0 (6)	0.669 8 (2)	H18	0.0226 (54)	0.8076 (65)	0.7884 (25)
C16	−0.236 3 (6)	0.735 1 (8)	0.671 0 (3)	H19	0.0440 (55)	0.6573 (66)	0.7099 (25)
C17	−0.250 1 (7)	0.824 9 (8)	0.718 1 (3)	H20	0.3859 (53)	0.5449 (64)	0.6752 (24)
C18	−0.151 7 (7)	0.849 1 (8)	0.761 9 (3)	H21	0.5552 (53)	0.5932 (65)	0.7419 (24)
C19	−0.039 0 (7)	0.784 6 (8)	0.759 6 (3)	H22	0.7145 (54)	0.4224 (62)	0.7521 (24)
C20	−0.025 5 (6)	0.695 7 (7)	0.714 2 (3)	H23	0.7022 (55)	0.2017 (64)	0.7014 (25)
C21	0.439 7 (5)	0.353 5 (7)	0.643 0 (2)	H24	0.5275 (54)	0.1647 (66)	0.6314 (25)
C22	0.448 9 (6)	0.475 3 (7)	0.678 2 (3)				

	β_{11}	β_{22}	β_{33}	β_{12}	β_{13}	β_{23}
Cu	0.0062 (1)	0.0109 (1)	0.0014 (1)	0.0011 (1)	0.0003 (1)	−0.0002 (1)
O1	0.0074 (4)	0.0148 (6)	0.0017 (1)	0.0024 (5)	0.0000 (1)	−0.0009 (2)
O2	0.0078 (4)	0.0129 (6)	0.0018 (1)	0.0026 (4)	−0.0000 (2)	−0.0010 (2)
O3	0.0064 (4)	0.0138 (6)	0.0018 (1)	−0.0001 (5)	0.0006 (1)	−0.0016 (2)
O4	0.0066 (4)	0.0127 (6)	0.0017 (1)	0.0009 (4)	0.0002 (1)	−0.0006 (2)
N1	0.0086 (5)	0.0126 (8)	0.0018 (1)	0.0012 (6)	0.0004 (2)	−0.0006 (3)
N2	0.0091 (6)	0.0153 (9)	0.0021 (1)	0.0005 (6)	−0.0003 (2)	−0.0017 (3)
C1	0.0067 (6)	0.0121 (9)	0.0016 (1)	−0.0008 (6)	0.0003 (2)	0.0010 (3)
C2	0.0078 (6)	0.0123 (9)	0.0017 (1)	0.0021 (7)	0.0003 (2)	−0.0002 (3)
C3	0.0083 (6)	0.0107 (9)	0.0016 (1)	0.0021 (6)	0.0007 (2)	0.0004 (3)
C4	0.0092 (6)	0.0125 (9)	0.0017 (1)	0.0036 (7)	0.0006 (2)	−0.0003 (3)
C5	0.0122 (8)	0.0094 (9)	0.0015 (1)	0.0013 (7)	0.0010 (3)	0.0003 (3)
C6	0.0139 (8)	0.0141 (10)	0.0023 (2)	0.0031 (9)	0.0010 (3)	−0.0013 (4)
C7	0.0124 (8)	0.0147 (12)	0.0021 (1)	−0.0009 (8)	0.0006 (3)	−0.0012 (3)
C8	0.0097 (7)	0.0177 (12)	0.0018 (1)	−0.0007 (8)	−0.0005 (3)	−0.0015 (3)
C9	0.0097 (7)	0.0195 (13)	0.0027 (2)	−0.0028 (8)	−0.0004 (3)	−0.0005 (4)
C10	0.0069 (6)	0.0113 (9)	0.0017 (1)	−0.0017 (6)	0.0000 (2)	0.0002 (3)
C11	0.0066 (6)	0.0138 (10)	0.0019 (1)	−0.0004 (6)	0.0008 (2)	−0.0004 (3)
C12	0.0061 (5)	0.0121 (9)	0.0017 (1)	0.0008 (7)	0.0005 (2)	0.0001 (3)
C13	0.0073 (6)	0.0114 (9)	0.0017 (1)	0.0001 (6)	0.0009 (2)	−0.0005 (3)
C14	0.0081 (6)	0.0100 (9)	0.0016 (1)	0.0005 (7)	0.0005 (2)	−0.0005 (3)
C15	0.0078 (6)	0.0105 (8)	0.0013 (1)	0.0004 (6)	0.0009 (2)	0.0003 (3)
C16	0.0088 (7)	0.0182 (12)	0.0020 (1)	0.0001 (8)	0.0008 (3)	−0.0017 (3)
C17	0.0119 (9)	0.0172 (12)	0.0032 (2)	0.0009 (9)	0.0020 (4)	−0.0013 (4)
C18	0.0151 (10)	0.0156 (11)	0.0018 (2)	0.0011 (9)	0.0014 (3)	−0.0004 (3)
C19	0.0139 (9)	0.0152 (11)	0.0019 (2)	0.0006 (8)	0.0003 (3)	−0.0008 (3)
C20	0.0107 (7)	0.0149 (11)	0.0017 (1)	0.0027 (7)	0.0001 (3)	−0.0006 (3)
C21	0.0065 (6)	0.0131 (9)	0.0016 (1)	−0.0003 (6)	0.0005 (2)	0.0010 (3)
C22	0.0080 (7)	0.0152 (10)	0.0021 (1)	−0.0006 (7)	0.0003 (3)	−0.0007 (3)
C23	0.0107 (8)	0.0231 (14)	0.0022 (2)	−0.0013 (10)	0.0003 (3)	−0.0009 (4)
C24	0.0106 (8)	0.0294 (17)	0.0018 (1)	−0.0024 (11)	0.0002 (3)	0.0002 (5)
C25	0.0093 (8)	0.0288 (17)	0.0026 (2)	0.0034 (10)	0.0000 (3)	0.0002 (5)
C26	0.0091 (7)	0.0194 (12)	0.0023 (2)	0.0025 (8)	−0.0005 (3)	−0.0008 (4)

^{a} Standard deviations from the full variance–covariance matrix are given in parentheses for the least significant digit(s). The form of the anisotropic temperature factor is $\exp[-h^2\beta_{11} + k^2\beta_{22} + l^2\beta_{33} + 2hk\beta_{12} + 2hl\beta_{13} + 2kl\beta_{23}]$. The isotropic temperature factor for all hydrogen atoms was set at 5.0.

indicate that, in fact, the parameters associated with magnetic exchange are nearly invariant in the binuclear triketonates of Co(II), Ni(II), and Cu(II) complexes. These data are summarized in Table VII. The major structural variant in terms of magnetic exchange is the M–M distance, which is undoubtedly a function of the size of the metal ion. It is likely that the 3.27–3.05 Å range in Table VII will bracket all divalent and trivalent first transition series metals. Another structural feature of the chelated 1,3,5-triketonates is the planarity of the triketonate moiety. In terms of magnetic exchange interactions, this is an important simplifying feature since any orbital-based interpretation of magnetic results will

Table III. Atomic Parameters for $Cu_2(BAA)_2(py)_2 \cdot 2py^a$

	x	y	z	B, Å²
Cu	0.0343 (2)	−0.0025 (1)	0.0789 (1)	
O1	0.0995 (11)	0.0513 (4)	0.1421 (5)	
O2	−0.0022 (14)	0.0474 (3)	0.0027 (7)	
O3	−0.1233 (11)	0.0585 (4)	−0.1336 (5)	
N	0.2217 (12)	0.0034 (5)	−0.1147 (5)	4.45 (24)
C1	0.0691 (18)	0.1007 (6)	0.1310 (8)	3.97 (36)
C2	0.0045 (16)	0.1241 (5)	0.0719 (8)	4.26 (34)
C3	−0.0314 (21)	0.0986 (6)	0.0078 (9)	4.67 (36)
C4	−0.0926 (17)	0.1279 (6)	−0.0497 (8)	4.16 (36)
C5	−0.1371 (20)	0.1056 (7)	−0.1133 (9)	5.22 (44)
C6	−0.2155 (19)	0.1424 (6)	−0.1671 (8)	5.89 (42)
C7	0.1157 (18)	0.1354 (6)	0.1952 (8)	4.35 (35)
C8	0.0526 (23)	0.1869 (7)	0.2007 (10)	8.18 (52)
C9	0.0909 (25)	0.2185 (8)	0.2607 (11)	10.11 (60)
C10	0.2008 (23)	0.1048 (8)	0.3115 (10)	8.84 (57)
C11	0.2604 (21)	0.1438 (7)	0.3065 (9)	6.98 (47)
C12	0.2092 (19)	0.1131 (6)	0.2466 (9)	5.77 (38)
C13	0.2643 (19)	−0.0217 (5)	−0.1750 (8)	4.69 (36)
C14	0.4244 (19)	−0.0230 (5)	−0.1960 (8)	5.22 (39)
C15	0.5372 (18)	0.0018 (7)	−0.1566 (7)	6.07 (34)
C16	0.4930 (19)	0.0279 (6)	−0.0954 (8)	6.36 (45)
C17	0.3315 (20)	0.0272 (6)	−0.0731 (8)	5.90 (40)
C18	0.5804 (30)	0.1673 (10)	0.1047 (12)	11.94 (74)
C19	0.6543 (28)	0.2140 (10)	0.0820 (14)	11.97 (70)
C20	0.6197 (30)	0.2325 (8)	0.0193 (13)	10.91 (72)
C21	0.5163 (33)	0.2113 (10)	−0.0198 (11)	11.84 (74)
C22	0.4407 (25)	0.1649 (10)	−0.0027 (13)	10.98 (69)
C23	0.4643 (28)	0.1430 (9)	0.0621 (13)	11.37 (69)

	β_{11}	β_{22}	β_{33}	β_{12}	β_{13}	β_{23}
Cu	0.0136 (3)	0.0013 (0)	0.0028 (1)	0.0004 (1)	−0.0002 (1)	−0.0003 (1)
O1	0.0147 (22)	0.0015 (2)	0.0036 (4)	0.0004 (6)	−0.0003 (8)	0.0004 (3)
O2	0.0157 (18)	0.0013 (2)	0.0035 (3)	−0.0001 (8)	0.0005 (6)	−0.0001 (4)
O3	0.0188 (23)	0.0015 (2)	0.0026 (4)	−0.0001 (6)	−0.0002 (8)	−0.0002 (2)

^{a} Anisotropic temperature factors of the form $\exp[-(h^2\beta_{11} + k^2\beta_{22} + l^2\beta_{33} + 2hk\beta_{12} + 2hl\beta_{13} + 2kl\beta_{23})]$ were used for the Cu(II) ion and oxygen atoms. Standard deviations of the last significant figure given in parentheses are given in this table. Atoms C18–C23 are the pyridine of solvation.

Table IV. Deviations of Atoms from Mean Planes (Å)

$Cu_2(DTFACP)_2$- $(H_2O)_2 \cdot H_2O$		$Cu_2(BAA)_2$- $(py)_2 \cdot 2py^a$		$[CuH_2(BAA)_2en]_2$	
Cu1	−0.10	Cu	0.23	Cu	−0.26
Cu2	−0.9	Cu'	−0.23	O1	−0.07
O1	−0.08	O1	−0.06	O2	−0.37
O2	0.16	O2	−0.11	O3	−0.05
O3	−0.04	O3	−0.03	O4	−0.24
O4	0.25	C1	−0.04	N1	0.02
O5	−0.41	C2	−0.03	N2	−0.18
O6	−0.34	C3	0.00	C1	0.17
C1	0.19	C4	0.04	C2	0.15
C2	0.01	C5	0.06	C3	0.03
C3	−0.01	O1'	0.06	C4	0.08
C4	0.14	O2'	0.11	C5	0.11
C5	0.11	O3'	0.03	C7	0.11
C6	0.02	C1'	0.04	C8	0.11
C7	−0.07	C2'	−0.03	C10	0.04
C8	0.05	C3'	0.00	C11	0.28
C9	−0.05	C4'	−0.04	C12	0.07
C10	−0.01	C5'	−0.06	C13	0.35
C11	0.28			C14	0.26
C12	0.32				
C13	0.01				
C14	−0.15				
C15	−0.06				
C16	0.29				
C18	0.22				
C19	0.16				

^{a} The primed atoms are symmetry related to the unprimed atom by the inversion center at origin of the cell.

be facilitated by simple geometry.

In discussions of the influence of the unpaired electron symmetry on the magnetic exchange in binuclear d^9–d^9 systems, it is instructive to focus on a number of different

Table V. Temperature-Dependent Magnetism of the Dimer $[CuH_2(BAA)_2en]_2$

T, K	$10^6 x'_m$, cgsu	μ_{eff}, μ_B	T, K	$10^6 x'_m$, cgsu	μ_{eff}, μ_B
4.5	56 910	1.43	13.0	35 020	1.91
5.0	57 400	1.52	15.0	30 900	1.93
5.5	55 870	1.57	19.0	21 140	1.79
6.0	53 550	1.60	24.0	17 260	1.82
7.0	56 660	1.78	77	5 000	1.76
9.0	43 520	1.77	195	2 130	1.82
10.0	40 690	1.81	273	1 520	1.82
11.0	38 370	1.84	297	1 450	1.86
12.0	36 310	1.87			

Table VI. Magnetic Properties of $[Cu_2(DTFACP)_2(H_2O)_2]_2 \cdot 2H_2O$ as a Function of Temperature^a

T, K	10^6- $(x'_m - N\alpha)$,^{b} cgsu	μ_{eff},^{c} μ_B	$10^6 x'_m$- (cor),^{d} cgsu	$10^6 x'_m$- (calcd),^{e} cgsu
77	195	0.35	45	~0
195	89	0.37	26	35
273	160	0.59	115	115
297	187	0.67	140	140
333	226	0.78	186	180
350	260	0.85	225	200
393	225	0.84	180	230

^{a} All values are on a per Cu(II) basis. ^{b} Assuming $N\alpha \cong 100 \times 10^{-6}$ cgsu. ^{c} $\mu_{eff} = 2.83[(x'_m - N\alpha)T]^{1/2}$. ^{d} Corrected x'_m, which has been corrected assuming a 3% paramagnetic impurity. ^{e} Calculated using the Bleaney–Bowers equation with $g = 2.12$ and $J = -370$ cm^{-1}.

structural types. In Figure 15, generalized structures of binuclear copper(II) complexes are represented for square-planar, square-pyramidal, and distorted octahedral geometries,
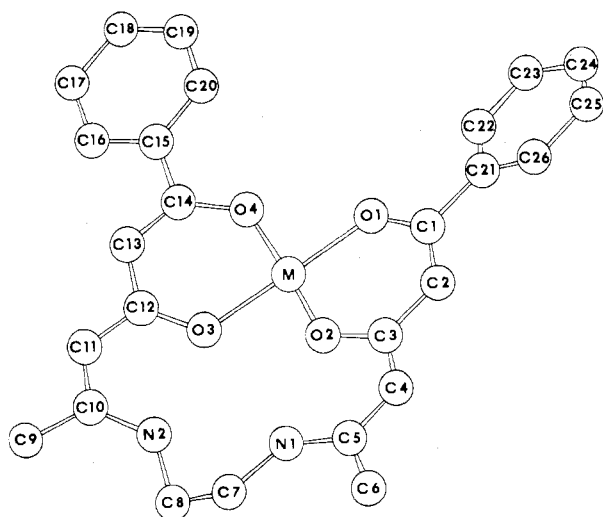
Figure 10. Molecular structure and atomic labeling of [CuH$_2$-(BAA)$_2$en]$_2$.

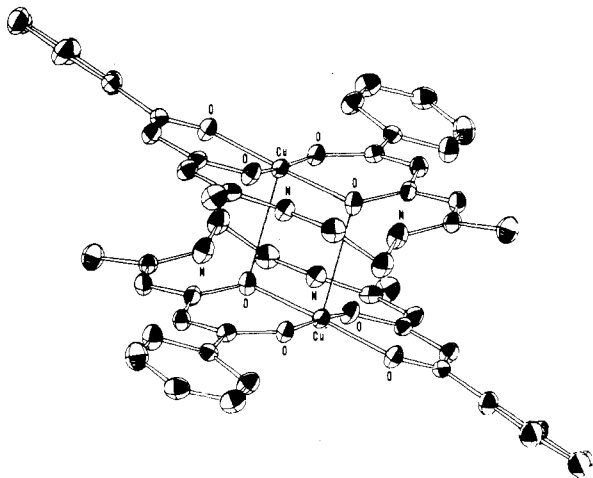**Figure 11.** Structure of the [CuH$_2$(BAA)$_2$en]$_2$ dimer with thermal ellipsoids.
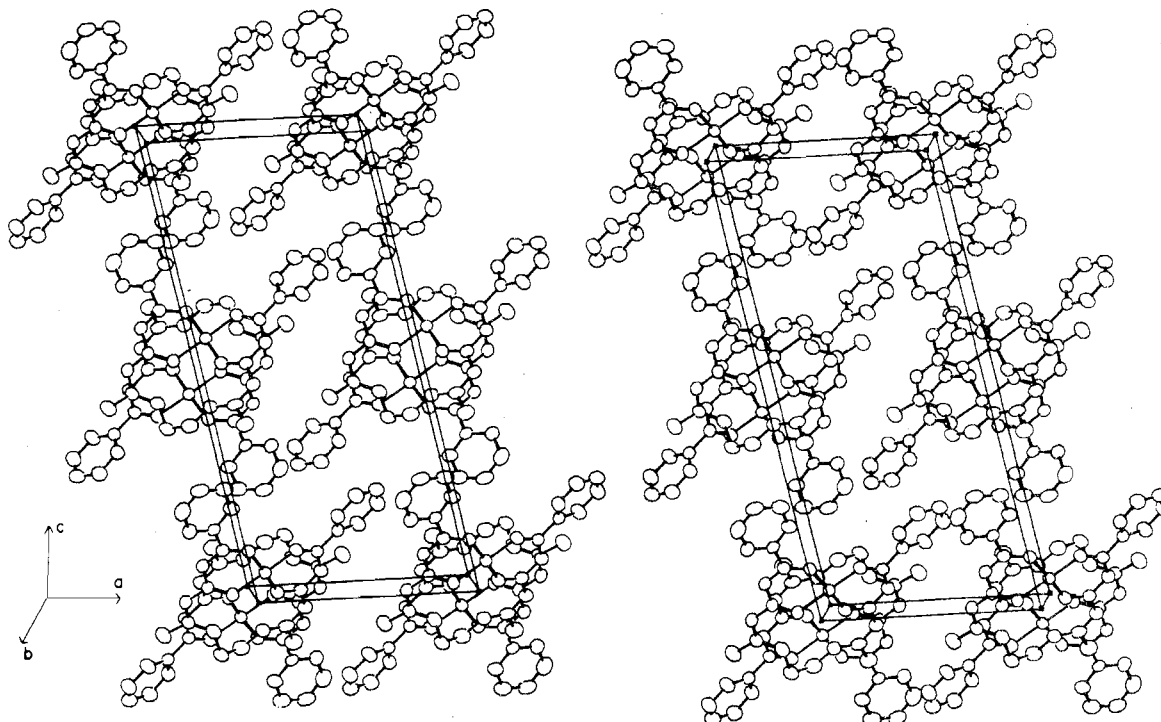
which are the geometries most often observed in these complexes. The magnetic plane in each Cu(II) ion can be defined as the plane of the four most strongly bound ligands since the unpaired electron exists in this plane. In structures a and b the interacting planes are coplanar, the simplest geometry for correlating structure and magnetism. In structures c and d there may be direct interaction between two magnetic planes, but the interacting planes are not coplanar. The angle α_d is the dihedral angle between the magnetic planes. Structure e is a distinctly different case in which the magnetic planes are parallel and magnetic interaction depends upon copper having a coordination number greater than 4. Although compounds of structures b, c, d, or e could each contain Cu–X–Cu bridging angles of 90°, it is unlikely that they would all exhibit similar magnetic exchange interactions as is often presumed.

By far the most common Cu(II) binuclear species are the dibridged structures b, d, and e. Of these, the most complete structural and magnetic studies have been carried out on complexes of general structure b.[3,15-21] One reason for this interest is the search for a clear relationship between the size of the bridging angle and the size and magnitude of the exchange constant, J. Hatfield, Hodgson, and co-workers[15-18] have characterized a number of hydroxo-bridged Cu(II) complexes and have successfully correlated the Cu–O–Cu bridging angle with the sign and magnitude of the exchange constant. They found parallel spin coupling at angles less than 98° and antiparallel coupling at angles greater than 98°. The plot of J vs. the size of the bridging angle is relatively linear.[18] The correlation appears to be valid only as long as the bridging groups are ⁻OH and the structure is close to b which suggests that other parameters are important as well as the bridging angle. The available data do not allow one to identify these parameters with certainty, but it is logical to assume that the orientation of the magnetic planes and distortions from coplanarity would play important roles.

One clear example of the importance of distortion is found in the binuclear complexes studied by Sinn and Robinson[21] in which the basic structure type is b but the Cu(II) geometries are distorted from planar toward tetrahedral. These complexes

Figure 12. Packing diagram of [CuH$_2$(BAA)$_2$en]$_2$.

Table VII. Interatomic Distances and Angles in Metal Coordination Spheres of 1,3,5-Triketonates

	Distances, Å				Angles, deg				
Compd	M–M	O_b–O_b	O_t–O_b	O_t–O_t	O_t–M–O_t	O_t–M–O_b	O_b–M–O_b	M–O_b–M	Ref
$Co_2(DBA)_2(py)_4$[a]	3.27	2.62	2.85	3.22	106.6	88.1	77.3	102.7	1
$Ni_2(DBA)_2(py)_4$[a]	3.17	2.59	2.85	3.13	102.2	89.6	78.5	101.5	2
$Cu_2(BAA)_2(py)_2$	3.05	2.46	2.77	2.81	94.3	92.8	76.6	103.4	This work
$Cu_2(DTFACP)_2(H_2O)_2$	3.06	2.37	2.78	2.89	98.8	92.5	75.1	103.7	This work
$Cu_2(DAA)_2(py)_2$[b]	3.05	2.41	2.78	2.80	94	93	77	103	3

[a] DBA^{2-} is the dianion of 1,5-diphenyl-1,3,5-pentanetrione (dibenzoylacetone). [b] DAA^{2-} is the dianion of 2,4,6-heptanetrione (diacetylacetone).

Table VIII. Magnetic and Structural Parameters for Several Binuclear Copper(II) Complexes with Bridging Oxygens

Compd	Structure type (Figure 1)	Cu–O–Cu, deg	Cu–Cu, Å	Type of bridge oxygen	J, cm^{-1}	Ref
$[Cu(tmen)OH]_2Br_2$	b	104.4	3.00	Hydroxide	−255	18
$[Cu(teen)OH]_2(ClO_4)_2$	b	103.0	2.98	Hydroxide	−205	29
$[Cu(C_8H_{10}N_2O)]_2$	b	103.9	3.00	Alkoxide	−280	19
$Cu_2(cbpb)_2Br_2$	b[a]	101.2	3.02	Phenolic	−220	21b
$Cu_2(cbpb)_2Cl_2$	b[a]		3.04	Phenolic	−146	21b
$Cu_2(DAA)_2(py)_2$	b	103	3.05	Ketonic	−345	3
$Cu_2(DTFACP)_2(H_2O)_2$	b	103.8	3.06	Ketonic	−370	This work
$Cu_2(BAA)_2(py)_2$	b	103.5	3.06	Ketonic	−370	This work
$[Cu(pyO)_2(NO_3)_2]_2$	e	102.9	3.46	N-Oxide	+7.5	15

[a] The two copper and two oxygen atoms lie in a plane, but the other ligands L are tetrahedrally displaced.

exhibit much weaker antiferromagnetic interactions than otherwise might be expected, a fact which the authors attribute to the tetrahedral distortion.

Another type of distortion from b is a nonzero dihedral angle between the two copper coordination planes. As this distortion increases, structure type d results. The hydroxo-bridged complex $[Cu(bpy)OH]_2SO_4 \cdot 5H_2O$ has this type of distortion with a dihedral angle of 7.9°.[22] The Cu–O–Cu bridging angle is 97°. The magnetic exchange is reported to be ferromagnetic with $J = +24$ cm^{-1}.[22] The structure of $[Cu(bpy)OH]_2SO_4 \cdot 5H_2O$ is very similar to that of the binuclear complex containing the ligand formed from picolinic acid and 3-aminopropanol which has a dihedral angle of 15.9° and a bridging angle of 98.3°.[23] The similarities are, however, not transferred to the magnetic properties since Bertrand, Fujita, and Eller[23] reported an antiferromagnetic exchange with $J = -65$ cm^{-1}. The importance of the noncoplanarity between the two magnetic planes is not known; however, one would expect that as the dihedral angle increases, it would have a profound effect on the exchange mechanism.

Many data exist for dimers of structure e which may be described as two weakly bridged, parallel magnetic planes.[24–26] The coupling in such systems is apparently always weak and may be either ferromagnetic or antiferromagnetic.[24] In all cases, the Cu–Cu distance is large and the bridging angle is usually in the 90–100° range. This is certainly a case in which the parallel orientation of the magnetic planes is more important in determining magnetic exchange than is the bridging angle. This is strikingly demonstrated for $[Cu(pyNO)_2(NO_3)_2]_2$[24] with structure type e and $Cu_2(DAA)_2(py)_2$[3] with structure type b, both of which have bridging angles of 103°. In the former $J = +5$ cm^{-1} and in the latter $J = -345$ cm^{-1}. Clearly, the orientation of the magnetic planes and not the bridging angle is the determining factor in such cases.

In addition to these purely structurally considerations, the nature of the bridging atom is also important. This is clearly illustrated by a comparison of the magnetic properties of hydroxo-bridged $[Cu(teen)OH]_2(ClO_4)_2$[29] and of Cu_2-

$(BAA)_2(py)_2$ which is reported herein and contains a keto oxygen. Both compounds have the planar structure b and the Cu–O–Cu angles are 103.0 and 103.5°, respectively. In spite of these similarities, the value of J for $[Cu(teen)OH]_2(ClO_4)_2$ is −205 cm^{-1} while for $Cu_2(BAA)_2(py)_2$ $J = -370$ cm^{-1}. The most obvious difference between the bridging systems in the two is an −OH oxygen vs. a ketonic oxygen bridging atom.

More complex situations frequently arise through dimerization of binuclear moieties resulting in tetranuclear species. Depending upon the orientation of two binuclear molecules, either a staggered or a cubane arrangement is achieved in the tetranuclear molecule. The staggered arrangement has been observed for a Schiff base complex[27,28] and the cubane structure for a 1,3-diketo imino alcohol.[20] Schematics of these structures are shown as

staggered

cubane type
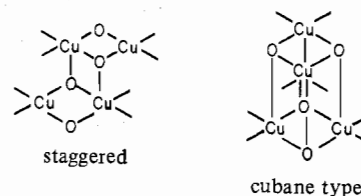
To a first approximation, the two structures are related to one another by a 90° rotation of one binuclear moiety. The magnetic properties of the two appear considerably different, although the data are incomplete for the cubane structure. The molecule with the staggered arrangement has a magnetic moment of about 1.58 μ_B at 300 K and 0.6 μ_B at 100 K whereas the cubane molecule has a normal moment of 1.84 μ_B at room temperature. Bertrand and Kelley[20] have attributed the normal moment of the cubane molecule to the fact that the bridging oxygens are tetrahedrally hybridized, precluding π bonding.

It is apparent from the above discussion that no single structural parameter (such as the bridging angle) can account for the magnetic properties in polynuclear complexes, the relative simplicity of d^9–d^9 systems notwithstanding.
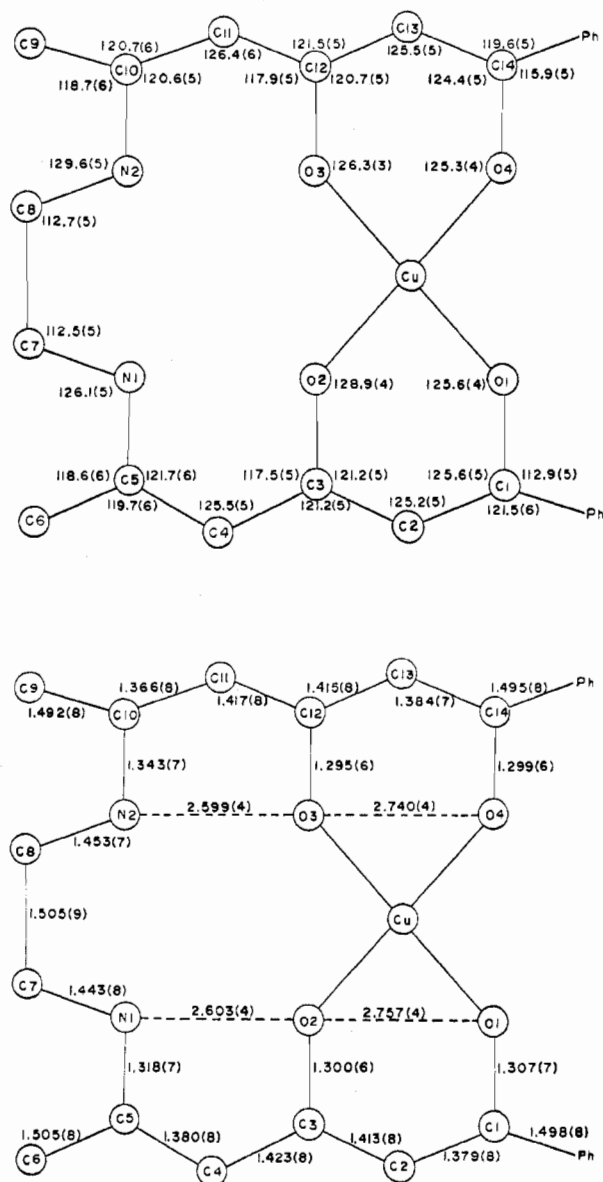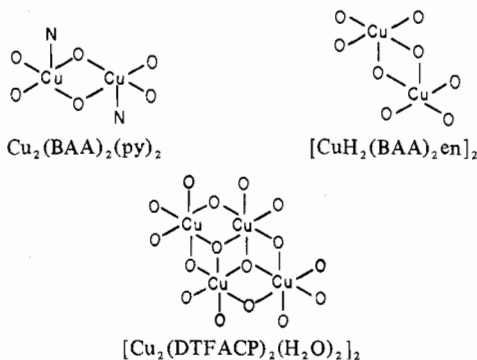
Figure 13. Distances and angles in the ligand of [CuH$_2$-(BAA)$_2$en]$_2$.

The three compounds discussed herein represent a graphic illustration of the importance of the magnetic plane orientation on the magnetic exchange in binuclear Cu(II) complexes. The generalized coordination spheres are shown by

Cu$_2$(BAA)$_2$(py)$_2$ [CuH$_2$(BAA)$_2$en]$_2$

[Cu$_2$(DTFACP)$_2$(H$_2$O)$_2$]$_2$

The complex Cu$_2$(BAA)$_2$(py)$_2$ has structure type b and only the potential for in-plane exchange between coplanar magnetic planes. This compound is strongly antiferromagnetic with J = −370 cm^{-1}. The mononuclear dimer [CuH$_2$(BAA)$_2$en]$_2$ has an e type structure and the potential only for exchange between
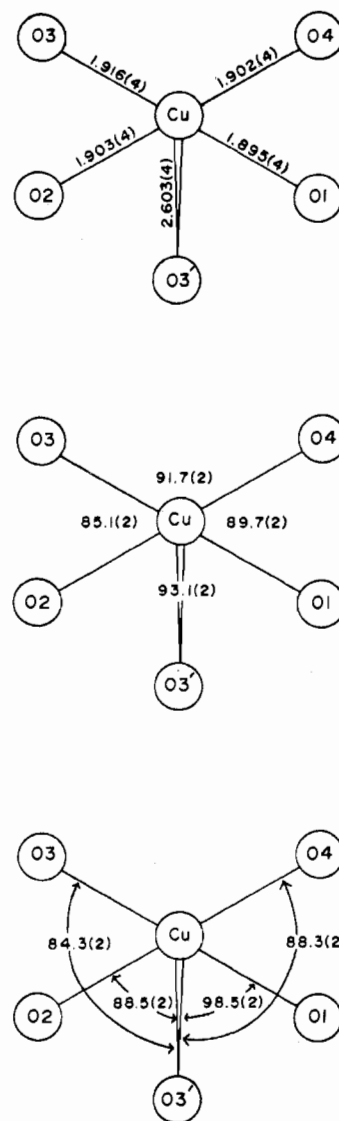
Figure 14. Distances and angles in the coordination sphere of [CuH$_2$(BAA)$_2$en]$_2$.

parallel magnetic planes. As a result, the exchange is very weak and for practical purposes $J \simeq 0$. Extremely weak out-of-plane exchange is consistent with results obtained by Hatfield, Hodgson, and co-workers for other systems.[15,25,30] The binuclear dimer [Cu$_2$(DTFACP)$_2$(H$_2$O)$_2$]$_2$ has a staggered arrangement made up of a combination of structures b and e. The tetranuclear complex is strongly antiferromagnetic with J = −370 cm^{-1}. The similarities between the magnetic properties of [Cu$_2$(DTFACP)$_2$(H$_2$O)$_2$]$_2$ and Cu$_2$-(BAA)$_2$(py)$_2$ are due to the structural and bonding similarities of the binuclear moieties. As in CuH$_2$(BAA)$_2$en, the out-of-plane exchange in [Cu$_2$(DTFACP)$_2$(H$_2$)$_2$]$_2$ is negligibly small.

In Table VIII the bridging angles, Cu–Cu distances, types of bridging atoms, and magnetic properties of several binuclear Cu(II) complexes are compared. All of the compounds in Table VIII have bridging angles very close to 103° and all except [Cu(pyO)$_2$(NO$_3$)$_2$]$_2$ have the generalized structure b (Figure 15). For those of structure b, the value of J varies by more than a factor of 2 even though the bridging angles and Cu–Cu distances are nearly equal. Thus, it appears that the nature of the bridging oxygen is of considerable importance.

One could argue from the data in Table VIII that the increased Cu–Cu distance in [Cu(pyO)$_2$(NO$_3$)$_2$]$_2$ (and in

A. Direct Interaction Between Magnetic Planes

Coplanar Magnetic Planes

Non-coplanar Magnetic Planes
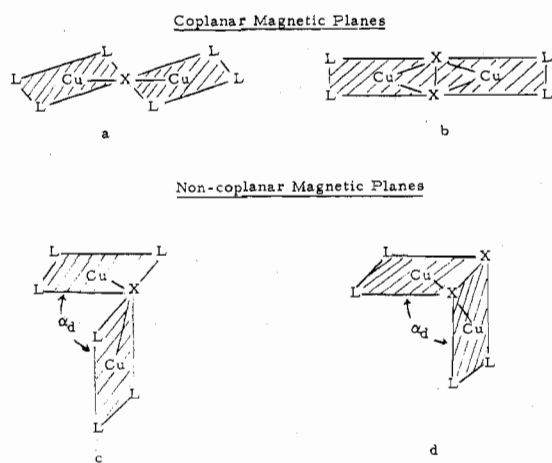
B. Indirect Interaction Between Magnetic Planes

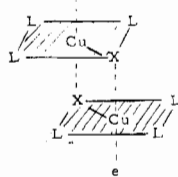**Figure 15.** Most probable orientation of magnetic planes for binuclear Cu(II) complexes.

$[CuH_2(BAA)_2en]_2)$ is the reason for the weak exchange rather than the parallel orientation of magnetic planes. However, an oxime-bridged binuclear complex with coplanar magnetic planes reported by Bertrand, Smith, and Eller[31] has a Cu–Cu distance of 3.58 Å and is diamagnetic at room temperature ($|J| > 700$ cm^{-1}). Thus, the orientation of the magnetic planes rather than the bridging angle or the metal–metal distance is most important. In other words, the relative symmetry of the exchanging electrons is the most critical feature. The nature of the bridging atom(s) appears to play a secondary role determining the value of J, with the value of the bridging angle a further perturbation.

One additional comment concerning the structure and magnetism of binuclear 1,3,5-triketonates should be mentioned. This deals with the fact that the bond angles about the Cu(II) ions are significantly distorted from 90°. The O_b–Cu–O_b angles in the four-membered Cu–O ring are about 75°. Since magnetic exchange takes place in this ring, orbital explanations are complicated by such distortion. The bond angle of 75° must result in some significant interaction of both atomic d orbitals in the xy plane with the bridging oxygens rather than just one as would be expected if the angle were 90°. The effect of this on magnetic exchange is not known.

The importance of the orientation of the magnetic planes in polynuclear copper(II) complexes is, of course, a function of the spatial orientation of the unpaired electron on each copper relative to any neighbors which are able to interact magnetically. In this regard, it would be interesting to apply this argument both to polynuclear copper complexes with more than two coppers per molecule and to polynuclear complexes of other metal ions which contain unpaired electrons with

different spatial orientations but in similar ligand environments.

References and Notes

(1) J. M. Kuszaj, B. Tomlonovic, D. P. Murtha, R. L. Lintvedt, and M. D. Glick, *Inorg. Chem.*, **12**, 1297 (1973).
(2) R. L. Lintvedt, L. L. Borer, D. P. Murtha, J. M. Kuszaj, and M. D. Glick, *Inorg. Chem.*, **13**, 18 (1974).
(3) A. B. Blake and L. R. Fraser, *J. Chem. Soc., Dalton Trans.*, 2554 (1974).
(4) B. Tomlonovic, R. L. Hough, M. D. Glick, and R. L. Lintvedt, *J. Am. Chem. Soc.*, **97**, 2925 (1975).
(5) M. D. Glick, R. L. Lintvedt, D. Gavel, and B. Tomlonovic, *Inorg. Chem.*, **15**, 1654 (1976).
(6) R. L. Lintvedt and J. L. Mack, 6th Central Regional Meeting of the American Chemical Society, Detroit, Mich., April 1974, paper 613.
(7) M. D. Glick and R. L. Lintvedt, *Prog. Inorg. Chem.*, **21**, 233 (1976).
(8) J. B. Goodenough, "Magnetism and the Chemical Bond", Interscience, New York, N.Y., 1963, p 180 ff.
(9) M. L. Miles, T. M. Harris, and C. R. Hauser, *J. Org. Chem.*, **30**, 1007 (1965).
(10) D. P. Murtha and R. L. Lintvedt, *Inorg. Chem.*, **9**, 1532 (1970).
(11) B. N. Figgis and J. Lewis in "Modern Coordination Chemistry", J. Lewis and R. G. Wilkins, Ed., Interscience, New York, N.Y., 1960.
(12) Local versions of the following programs were used: SYNCOR, W. Schmonsees' data reduction program; DACOR, D. Smith's data reduction program; FORDAP, A. Zalkin's Fourier program; ORFLS and ORFFE, W. Busing, K. Martin, and H. Levy's full-matrix, least-squares and function and error programs; ORTEP, C. K. Johnson's plotting program; HFINDER, A. Zalkin's hydrogen atom finding program. In the last program, the C–H distance was assumed to be 0.97 Å. An interactive graphics package written in our laboratory for a Data General NOVA-1200 computer and an Owens-Illinois Plasma Display Panel was used. Scattering factors for Cu^{2+} and other atoms were taken from J. A. Ibers and W. C. Hamilton, Ed., "International Tables for X-Ray Crystallography", Vol. IV, Kynoch Press, Birmingham, England, 1974.
(13) Supplementary material.
(14) B. Bleaney and K. D. Bowers, *Proc. R. Soc. London, Ser. A*, **214**, 451 (1952).
(15) K. T. McGregor, D. J. Hodgson, and W. E. Hatfield, *Inorg. Chem.*, **12**, 731 (1973).
(16) D. L. Lewis, W. E. Hatfield, and D. J. Hodgson, *Inorg. Chem.*, **13**, 147 (1974).
(17) D. L. Lewis, W. E. Hatfield, and D. J. Hodgson, *Inorg. Chem.*, **11**, 2216 (1972).
(18) K. T. McGregor, N. T. Watkins, D. L. Lewis, R. F. Drake, D. J. Hodgson, and W. E. Hatfield, *Inorg. Nucl. Chem. Lett.*, **9**, 423 (1973).
(19) J. A. Bertrand and C. E. Kirkwood, *Inorg. Chim. Acta*, **6**, 248 (1972).
(20) J. A. Bertrand and J. A. Kelley, *Inorg. Chim. Acta*, **4**, 203 (1970).
(21) (a) E. Sinn and W. T. Robinson, *J. Chem. Soc., Chem. Commun.*, 359 (1972); (b) P. Gluvchinsky, G. M. Mockler, P. C. Healy, and E. Sinn, *J. Chem. Soc., Dalton Trans.*, 1156 (1974).
(22) A. T. Casey, B. F. Hoskins, and F. D. Whillans, *Chem. Commun.*, 904 (1970); J. A. Barnes, D. J. Hodgson, and W. E. Hatfield, *Inorg. Chem.*, **11**, 144 (1972).
(23) J. A. Bertrand, E. Fujita, and P. G. Eller, *Inorg. Chem.*, **13**, 2067 (1974).
(24) W. E. Hatfield, *Inorg. Chem.*, **11**, 216 (1972), and references therein.
(25) P. Singh, D. Y. Jeter, W. E. Hatfield, and D. J. Hodgson, *Inorg. Chem.*, **11**, 1657 (1972).
(26) G. W. Inman, W. E. Hatfield, and R. F. Drake, *Inorg. Chem.*, **11**, 2425 (1972); E. D. Estes, W. E. Estes, R. P. Scaringe, W. E. Hatfield, and D. J. Hodgson, *ibid.*, **14**, 2564 (1975).
(27) G. A. Barclay and G. F. Hoskins, *J. Chem. Soc.*, 1979 (1965).
(28) W. E. Hatfield and G. W. Inman, Jr., *Inorg. Chem.*, **8**, 1376 (1969).
(29) E. D. Estes, W. E. Hatfield, and D. J. Hodgson, *Inorg. Chem.*, **13**, 1654 (1974).
(30) W. E. Hatfield, *Inorg. Chem.*, **11**, 216 (1972).
(31) J. A. Bertrand, J. H. Smith, and P. G. Eller, *Inorg. Chem.*, **13**, 1649 (1974).